

ILLUMINATED, AND ENLIGHTENED, BY GRB 991216

M. VIETRI

Università di Roma 3, Via della Vasca Navale 84, I-00147 Roma, Italy; e-mail: vietri@fis.uniroma3.it
G. GHISELLINI AND D. LAZZATI¹

Osservatorio Astronomico di Brera, Via E. Bianchi 46 I-23807 Merate, Italy; e-mail: gabriele@merate.mi.astro.it

F. FIORE AND L. STELLA

Osservatorio Astronomico di Roma, Via Frascati 33, I-00040 Monteporzio Catone, Italy; e-mail: fiore.stella@comap.mporzio.astro.it

Draft version October 24, 2018

ABSTRACT

We consider models for the generation of the emission line recently discovered in the X-ray afterglow spectrum of several bursts, and especially of GRB 991216 observed by *Chandra*. These observations suggest the presence of 0.1–1 solar masses of iron in the vicinity of the bursts. We show that there are strong geometrical and kinematical constraints on the line emitting material. We discuss several classes of models, favoring one where the line photons are produced by reflection off the walls of a wide funnel of semi-opening angle $\vartheta \approx 45^\circ$ excavated in a young (a few months old) supernova remnant made of $\approx 10M_\odot$ with radius 6×10^{15} cm, and $\approx 1M_\odot$ of iron, providing strong support for the SupraNova model.

Subject headings: gamma rays: bursts — radiation mechanisms: nonthermal — line: formation

1. INTRODUCTION

There are now five bursts with evidence for large amounts of material around the site of the explosion: four (GRB 970508, Piro et al., 1999; GRB 970828, Yoshida et al., 1999; GRB 991216, Piro et al., 2000, hereafter P2000; GRB 000214, Antonelli et al., 2000) show an emission feature during the afterglow, and one (GRB 990705, Amati et al., 2000) displays an edge in absorption during the burst itself. The observations of GRB 991216 by *Chandra*, begun 37 hr after the burst and lasting for about 3 hr, show a 3.49 ± 0.06 keV line significant at a $\sim 4\sigma$ level. If the line is identified with the recombination $K\alpha$ line from H-like iron (6.97 keV), the inferred redshift is $z = 1.00 \pm 0.02$ consistent with the largest optical absorption redshift system ($z = 1.02$) (Vreeswijk et al., 2000). The line, resolved by *Chandra*, displays a width corresponding to $0.05c$ (P2000). The line and the 2–10 keV continuum fluxes were $\sim 1.6 \times 10^{-13}$ and $\sim 2.4 \times 10^{-12}$ erg s⁻¹ cm⁻², respectively, implying (for $z = 1.02$) an emission rate of iron line photons of $\dot{N}_{\text{line}} \simeq 4 \times 10^{52}$ s⁻¹, luminosity $L_{\text{line}} \simeq 4 \times 10^{44}$ erg s⁻¹ and total energy $E_{\text{line}} \sim 3 \times 10^{49}$ erg (assuming steady emission for $40/(1+z)$ hr, with $H_0 = 75$ km s⁻¹ Mpc⁻¹ and $q_0 = 0.5$). If each iron atom produces k line photons, the required iron mass is $M_{\text{Fe}} \simeq 195 k^{-1} M_\odot$. Bringing this mass down to $\sim 0.1 M_\odot$ implies $k > 2000$ which in turn implies a limit on the recombination time ². This translates into the condition $n_e > 10^{10} T_7^{3/4}$ cm⁻³; the electron temperature $T = 10^7 T_7$ K comes from interpreting the broad bump, marginally detected by *Chandra*, at 4.4 ± 0.5 keV as the recombination continuum of H-like iron (9.28 keV). Analogously to GRB 950708 (Lazzati et al. 1999), the line detection implies the presence of $\approx 0.5M_\odot$ of pure iron in the vicinity of the burster.

Observation of the line t_{obs} after the burst implies that the line emitting material must be within $\sim ct_{\text{obs}}/(1+z)$ from the burst site: this region must then be compact, contain $\sim 0.1M_\odot$ only

in iron, but nevertheless be optically thin to electron scattering, such that Comptonization does not broaden the line beyond the observed width. We call this the *size problem*.

Furthermore, if we interpret the line width as due to the velocity of a supernova remnant, the limit on the size allows to estimate the age of the remnant: for GRB 991216, ~ 15 days. At this time (Fig. 1), cobalt nuclei outnumber nickel and iron nuclei and the line would be produced mainly by cobalt, not iron, at an energy $\epsilon = 7.5/(1+z)$ keV. We call this the *kinematic problem*.

We discuss in section 2 the constraints implied by the line observation; we then present in section 3 three scenarios which could produce the observed line. Two of them are found to be viable only by adopting ad hoc assumptions or through fine tuning, while a third scenario, the “wide funnel” scenario, appears to be more promising. In section 4 we discuss our results.

2. PHYSICAL AND GEOMETRICAL CONDITIONS

The detection of emission features in the afterglow spectra of GRBs some hours after the GRB event poses a strong constraint on the location of the line emitting material. If the line is detected after t_{obs} from the burst explosion the material must be located within a distance R given by

$$R \leq \frac{ct_{\text{obs}}}{1+z} \frac{1}{1-\cos\vartheta} \simeq \frac{1.1 \times 10^{15}}{1+z} \frac{t_{\text{obs}}}{10\text{h}} \frac{1}{1-\cos\vartheta} \text{ cm}, \quad (1)$$

where ϑ is the angle between the line emitting material and the line of sight at the GRB site. This limit has important implications, because the scattering optical depth is large,

$$\tau_T = \frac{\sigma_T M}{4\pi R^2 \mu m_p} \geq 54 \frac{(M/M_\odot)(1+z)^2(1-\cos\vartheta)^2}{\mu (t_{\text{obs}}/10\text{h})^2}, \quad (2)$$

(where $\mu = 1, 1.2$ and 2 for pure hydrogen, solar composition, and no hydrogen, respectively), and, for a remnant radial ve-

¹Present address: Institute of Astronomy, Madingley Road, Cambridge CB3 0HA, UK; e-mail: lazzati@ast.cam.ac.uk

²From the formulae given in Verner & Ferland (1996), the recombination time can be approximated by $t_{\text{rec}} \sim 12.7 T_7^{3/4} n_{10}^{-1}$ s in the temperature range $10^6 < T < 10^8$ K.

locity of $v = 10^9 v_9 \text{ cm s}^{-1}$ the time elapsed from the SN is $t_{\text{SN}} \simeq 12.5(t_{\text{obs}}/10\text{hr})/[(1+z)(1-\cos\vartheta)v_9]$ days, implying that most ^{56}Co nuclei (and a fraction of ^{56}Ni) have not yet decayed to ^{56}Fe (half-lives of 77.3 and 6.08 days, respectively). In Fig. 1 we show normalized abundances of nickel, cobalt and iron as a function of time from the SN explosion.

To produce the line by frequent recombinations and ionizations, a sufficiently high ionizing flux and a large number of H-like iron ions, FeXXVI, are required. Efficient use of these ions requires that the photoionization optical depth for FeXXVI, $\tau_{\text{FeXXVI}} \gtrsim 1$. Using photoionization cross section $\sigma_{\text{FeXXVI}} \sim 1.2 \times 10^{-20} \text{ cm}^2$, and abundance ratio $\xi = M_{\text{FeXXVI}}/M_{\text{Fe}}$, we have

$$\tau_{\text{FeXXVI}} = \frac{\sigma_{\text{FeXXVI}} \xi M_{\text{Fe}}}{56 m_p 4\pi R^2} = 2 \times 10^3 \frac{\xi}{R_{15}^2} \frac{M_{\text{Fe}}}{0.1 M_{\odot}}. \quad (3)$$

A strict *lower* limit on the ionizing continuum power comes from the line flux itself. For GRB 991216, for which there is no *rebusting* in the X-ray afterglow (contrary to GRB 970508), assuming an illumination time of 20 hr, we require $E_{\text{ion}} > 3 \times 10^{49} \text{ erg}$. Even in the case of an illuminating continuum not directly visible by us, we require that the scattered flux produced by the line emitting material does not affect the afterglow emission, i.e. it must contribute less than $10^{-12} \text{ erg cm}^{-2} \text{ s}^{-1}$ to the observed flux, giving the *upper* limit $\min(1, \tau_{\text{T}}) E_{\text{ion}} < 1.8 \times 10^{50} \text{ erg}$.

2.1. Compton broadening and Thomson optical depth

If the emitting atoms are diluted in an electron cloud, the fraction of unscattered flux $= [1 - \exp(-\tau_{\text{T}})]/\tau_{\text{T}}$, while if the scattering cloud surrounds a central source the fraction $= \exp(-\tau_{\text{T}})$. If the scattering electrons have a temperature in the $\sim 10^7 \text{ K}$ range (according to the indication that the recombination continuum observed in GRB991216 may be broad, P2000), the average energy shift of line photons scattered only once is $\Delta E/E \approx 0.063(kT/1 \text{ keV})^{1/2}$ (Pozdnyakov, Sobol & Sunyaev 1983), *already broader than the observed line width*. Multiple scatterings would further broaden the line, making it increasingly difficult to detect against the X-ray continuum. If the line of GRB 991216 were made by photons escaping unscattered from a medium with $\tau_{\text{T}} > 1$, the problem with the line flux would be exacerbated, a factor τ_{T} more iron being required.

An alternative possibility, that the electron temperature $\ll 10^7 \text{ K}$, say $\sim 10^6 \text{ K}$ expected if the ionizing continuum were steep and extended to low energies, might conjure with a suitable value of τ_{T} to yield, through Compton broadening, the observed line width. In this case, however, the centroid of the line would be redshifted (line photons are mostly backscattered by colder electrons) and the recombination continuum narrower. Due to poor statistics, the recombination continuum of GRB 991216 cannot place a firm constraint on the electron temperature, but the models in Section 3 are largely independent of the presence and width of the recombination emission continuum.

3. THE MODELS

We can roughly divide the models into *transmission* and *reflection* models. If we see the line in reflection, line photons come from the layer with $\tau_{\text{FeXXVI}} = \text{several}^3$. For an iron abundance greater than the solar value, in this layer $\tau_{\text{T}} \leq 1$. In general, transmission models require $\tau_{\text{T}} < 1$ and $\tau_{\text{FeXXVI}} \sim 1$, while

reflection models require $\tau_{\text{FeXXVI}} > \tau_{\text{T}}$. Each iron atom must produce ~ 2000 iron photons, and this requires an electron density larger than 10^{10} cm^{-3} .

The large equivalent widths of the X-ray line in GRB 991216 ($EW = 0.5 \text{ keV}$) and, especially, GRB 970508 ($EW \sim 1 \text{ keV}$), GRB 970828 ($EW \sim 3 \text{ keV}$) and GRB 000214 ($EW \sim 2 \text{ keV}$) favor models in which the line originates in reflection, not transmission. In reflection, in fact, the ionizing flux is always efficiently reprocessed in line photons in the $\tau_{\text{Fe}} \sim 1$ layer, while in transmission this happens only for a particular tuning of the FeXXVI and the free electron densities.

Three alternative geometries (Fig. 2) producing lines in reflection are described below.

In reflection models, we can derive the photon line luminosity by estimating the volume V_{em} effectively contributing to the line emission, and assuming a given iron mass. If the layer contributing to the emission has $\tau_{\text{T}} \sim 1$ (in order to avoid excessive Compton broadening of the line), and in this layer $\tau_{\text{FeXXVI}} \sim \text{a few}$ (to efficiently absorb the continuum), we have $V_{\text{em}} = S/(\sigma_{\text{T}} n_e)$, where S is the emitting surface. The line emission rate from V_{em} is then

$$\dot{N}_{\text{Fe}} = \frac{N_{\text{Fe}}}{t_{\text{rec}}} = \frac{S n_{\text{Fe}}}{1.3 \times 10^{11} T_7^{3/4} \sigma_{\text{T}}} \sim 3 \times 10^{53} \frac{(M_{\text{Fe}}/M_{\odot})}{T_7^{3/4} \Delta R_{15}} \text{ s}^{-1}. \quad (4)$$

where we assumed that the *total* volume is $V = S \Delta R$ (slab or shell geometry). Eq. 4 shows that the total iron mass must be a sizable fraction of a solar mass to obtain the observed line flux ($4 \times 10^{52} \text{ s}^{-1}$), but less than the largest observed values, $0.9 M_{\odot}$ for SN 1998bw (Type Ic, Sollerman et al., 2000) and SN1991T, (Type Ia, Filippenko et al., 1992). Eq. 4 all by itself establishes that the line emitting material must be a SNR: no other known astrophysical object contains so much iron, not even the largest known stars (though these fail by a factor of a few only).

Eq. 4 has another important implication: it fixes M/R , and since R is fixed (for a given geometry, see below) by the time-delay, the cloud density is also fixed, to within an order of magnitude. Solutions with densities much exceeding (or much below) $\approx 10^{10} \text{ cm}^{-3}$ are excluded.

3.1. The wide funnel

If the GRB explodes within the young remnant of a supernova, we must consider two possibilities: a plerionic and a shell remnant. In the first case, we consider a wide funnel excavated in a young plerionic remnant. This can solve the *size problem*, since it extends to large radii but, at the same time (Eq. 1), can maintain the time-delay contained because it is naturally built close to the polar axis (assumed close to the line of sight). The geometry is sketched in Fig. 2a. Fixing the line photons rate (Eq. 4) yields $R = 6 \times 10^{15} \text{ cm}$, and thus an opening angle $\vartheta = 48^\circ$, to fit the time-delay. For any reasonable SN composition, these parameters imply $n_e > 10^{10} \text{ cm}^{-3}$. The funnel walls are probably not straight (like in a cone geometry), but curved instead, like the surface of the coffee in a cup when it is spun up, and can be illuminated by the ionizing flux from a central source. Assuming a cone geometry for simplicity, we rewrite Equation 4 as

$$\dot{N}_{\text{Fe}} = 3.3 \times 10^{52} \frac{(M_{\text{Fe}}/M_{\odot})}{T_7^{3/4} (R_{15}/6)} \tan \vartheta \text{ s}^{-1}. \quad (5)$$

³What we call FeXXVI might well be CoXXVII or NiXXVIII, see section 2.

where in this case R (the radius of the filled remnant) has been used instead of ΔR and $\tan \vartheta$ takes into account the geometry of the funnel. This is a lower limit, since a parabolic geometry has a larger funnel surface and we neglected the (likely) density stratification inside the remnant.

Since the funnel's normal is *not* parallel to the incident photon's momentum, radiation pressure exerts a force parallel to the surface on the layer $\tau_T \leq 1$ (which reflects isotropically photons arriving from a specific direction). Calling φ the angle between the funnel's normal and the incident photon's arrival direction the absorbed fluence E_{ion} accelerates the funnel layer to a speed $v_f = \sin \varphi (2E_{\text{ion}}/M_{\text{layer}})^{1/2} \simeq 10^4 E_{\text{ion},50}^{1/2} \sin \varphi \text{ km s}^{-1}$ when $R = 6 \times 10^{15} \text{ cm}$. Thus, ablation by radiation pressure propels the reflecting layer to velocities like those seen in GRB991216 by P2000.

The funnel model can thus explain the observed line broadening even in a relatively old SNR. For a remnant with $v_{\text{ej}} = 3000 \text{ km s}^{-1}$, a typical value for type II SNe, we find a remnant age $t_{\text{SNR}} \sim 230$ days, enough to turn most ^{56}Ni and ^{56}Co into ^{56}Fe (Fig. 1). The emitting iron is then boosted to higher velocity by the ionizing flux, circumventing the kinematical problem.

3.2. Back of the remnant

We consider now a shell remnant, characterized by a wide opening, so that a substantial fraction of its inner face is visible (Fig. 2b), and illuminated by burst and afterglow and, more likely, by the shock due to the fireball impact (Böttcher 2000). Line photons are produced in the layer $\tau_{\text{FeXXVI}} \sim \text{few}$. As before, the remnant may have been expanding slowly, until accelerated by burst photons. Since we see the remnant's internal part, the *size* limit discussed in Section 2 is tighter, and we detect mainly redshifted photons. For a remnant distance $R = 10^{15} \text{ cm}$ and velocity $5,000 \text{ km s}^{-1}$, the age is ~ 20 days, close to the ^{56}Co peak (Fig. 1). However, the $7.5 \text{ keV } ^{56}\text{Co}$ line would be observed with a substantial redshift (and therefore mimic a $^{56}\text{Fe } 6.97 \text{ keV}$ line), if the burst photons increased the expanding velocity to $\sim 20,000 \text{ km s}^{-1}$ (implying that the burst emitted a few times 10^{52} erg sideways, for a $10 M_{\odot}$ remnant). In this model the observed line width of $15,000 \text{ km s}^{-1}$ requires that only a limited range of projections of the radial expansion velocity vectors are observed. This solution is not convincing since it involves fine tuning between the energy produced sideways and the mass of the remnant, in order to have the correct expansion velocity, even though it explains naturally the different centroid energy of the line observed in GRB 970508: since the line is redshifted by shell expansion, we expect a distribution of observed energies as a consequence of different velocities of the remnant.

3.3. Back-illuminated equatorial material

We now explore the possibility of a simultaneous GRB–“supernova” explosion. Consider a scenario in which the GRB ejects and accelerates a small amount of matter in a collimated cone, while a large amount of matter is instead ejected, at sub-relativistic speeds, along the progenitor's equator. For illustration, assume equal amounts of energy, 10^{52} erg , in both directions, and $1 M_{\odot}$ expelled along the equator. Then $v_{\text{eq}}/c = 0.148 E_{52}^{1/2} (M/M_{\odot})^{-1/2}$. Massive star progenitors are always surrounded by dense material from strong winds with mass

loss rates $\dot{m}_w = 10^{-5} \dot{m}_{w,-5}$ and velocity $v_w = 10^7 v_{w,7}$. This wind scatters back a fraction of the photons produced by the bursts and its afterglow (Thompson & Madau 2000), and, in return it is also accelerated until it reaches relativistic velocities, when scattering efficiency decreases. Thus assume that each electron (and the associated proton) scatters photons only until it reaches $\Gamma = 2$, i.e. until it has scattered a total energy of $m_p c^2$ (i.e. $\sim 2,000$ photons of 0.5 MeV each). In this case the scattered luminosity L_{scatt} is constant, since there are an equal number of electrons in a shell of constant width ΔR (for a density profile $\propto R^{-2}$). This luminosity is of the order:

$$L_{\text{scatt}} \sim m_p c^2 \frac{\dot{m}_w}{m_p v_w / c} = 1.8 \times 10^{45} \frac{\dot{m}_{w,-5}}{v_{w,7}} \text{ erg s}^{-1}. \quad (6)$$

Scattered photons illuminate the expanding equatorial matter after a time $2R/c$, producing X-ray line emission mostly due to $K\alpha$ emission from H-like ^{56}Ni at 8.1 keV . Even if the large expanding velocity makes the transverse Doppler shift important, this requires a fine tuned velocity to redshift the $8.1 \text{ keV } ^{56}\text{Ni}$ line into 6.97 keV , for which reason we consider this scenario unlikely.

4. CONCLUSIONS

X-ray line emission features from GRBs' afterglows give us information on the nature of their progenitors by imposing constraints on models, the most severe being how to arrange a large amount of line emitting material around the GRB site, but without large Thomson scattering opacities. A further limit comes from the line width of *Chandra*'s observation in GRB 991216. These observations require a large iron mass (Eq. 4), such as is seen only in SNe.

We have presented three distinct models: two (the “back of the remnant” and “back illuminated equatorial material” models) require that the observed emission line is produced by redshifted cobalt or nickel (instead of iron), and need fine tuning and/or ad hoc assumptions. The “wide funnel” model, instead, solves the size problem, and the acceleration of the line emitting material by grazing incident photons solves the kinematic problem, allowing time for cobalt to decay to iron. It implies that the GRB progenitors are massive stars exploded as supernovae months before the burst, contaminating the circum-burst environment with iron rich material. This two-step process, and the time-delay between the two steps, are predicted by the SupraNova scenario (Vietri & Stella, 1998). Alternative explanations invoke extremely iron enriched massive winds (Weth et al. 2000).

Future observations may address issues such as the presence of cobalt and nickel lines in the spectrum, the age of the remnant, the line profile, the geometry and kinematics of the emitting region, the presence of more than one line, the ionization state, the time evolution of the line and edges, all indicative of the characteristics of the illuminator. Together, this information may determine whether the line emitting material originates in a normal, albeit rare, supernova remnant or if a more exotic explosive phenomenon is required.

We thank Frits Paerels and Martin J. Rees for useful discussions.

REFERENCES

- Amati L., et al., 2000, *Science*, 290, 953
 Antonelli A. et al., 2000, *ApJ*, 545, L39
 Böttcher M., 2000, *ApJ*, 539, 102
 Filippenko, A.V., et al., 1992, *ApJ*, 384, L15
 Lazzati D., Campana S. & Ghisellini G., 1999, *MNRAS*, 304, L31.
 Piro L., et al., 1999, *ApJ*, 514, L73.
 Piro L., et al., 2000, *Science*, 290, 955 (P2000)
 Pozdnyakov L.A., Sobol I.M. & Sunyaev R.A., 1983, *Astroph. Space Phys. Rev.*, Vol 2, p. 189
 Sollerman J., Kozma C., Fransson C., Leibundgut B., Lundqvist P., Ryde F. & Woudt P., 2000, *ApJ*, 537, L127
 Thompson C. & Madau P., 2000, *ApJ*, 538, 105
 Verner D.A. & Ferland G.J., 1996, *ApJS*, 103, 467
 Vietri M. & Stella L., 1998, *ApJ.Lett.*, 507, L45.
 Vreeswijk P.M., et al., 2000, *GCN circular n.* 496.
 Yoshida, A., et al., 1999, *Astr. Ap. Suppl.*, 138, 433.
 Weth C., Meszaros P., Kallman T. & Rees M.J., 2000, *ApJ*, 534, 581

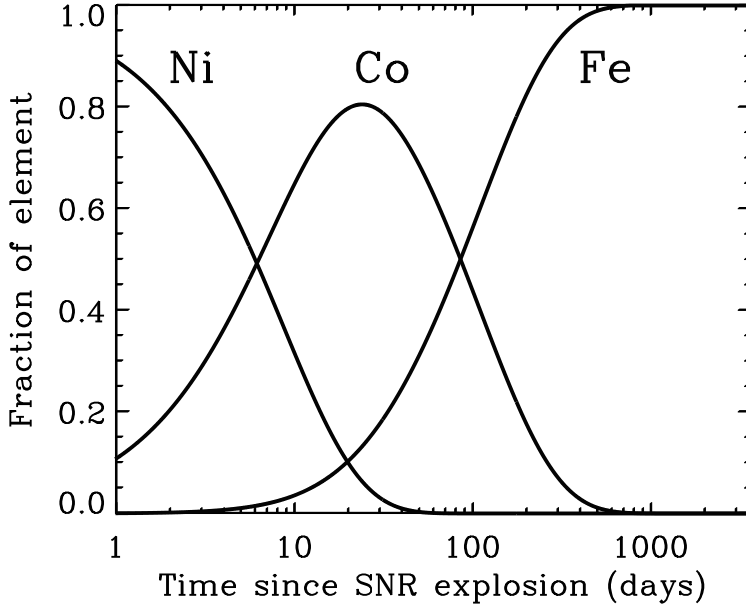


Fig. 1.— The normalized abundances of ^{56}Ni , ^{56}Co and ^{56}Fe as a function of time from the creation of ^{56}Ni . The neutral, He-like, H-like and recombination edge energies are (in keV): ^{56}Ni : 7.478, 7.806, 8.102, 10.775; ^{56}Co : 6.930, 7.242, 7.526, 10.012; ^{56}Fe : 6.404, 6.701, 6.973, 9.278.

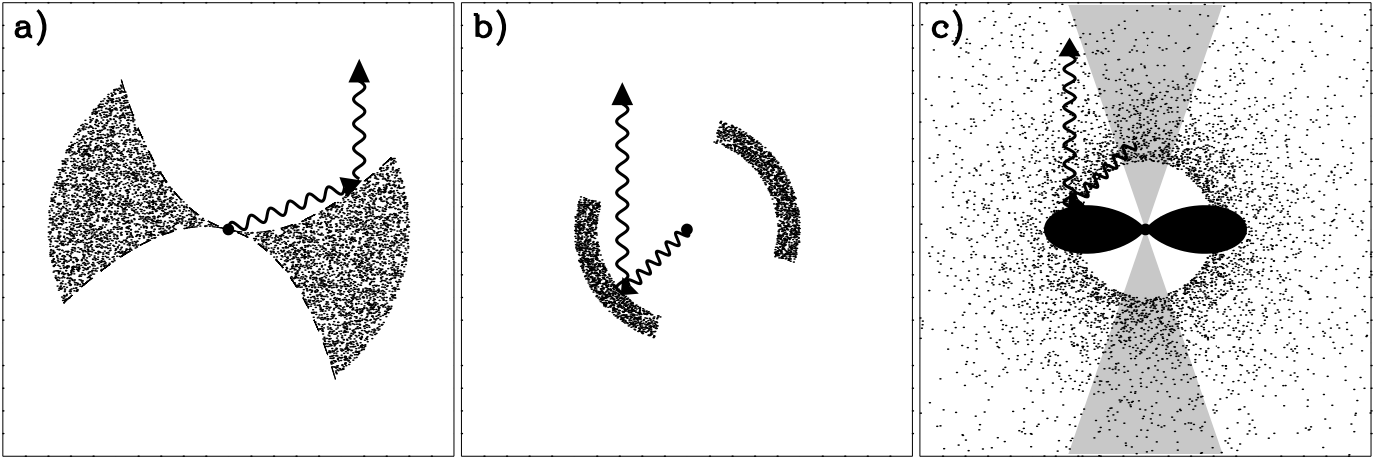


Fig. 2.— Cartoon of the three models discussed in this paper. In panel a) a funnel excavated in a supernova remnant produces the iron line in reflection, by material accelerated to $\sim 10,000 \text{ km s}^{-1}$ by the strong radiation pressure. In panel b) we see the internal parts of a young and receding supernova remnant, in panel c) some equatorial material exploding simultaneously with the burst is illuminated by burst and afterglow photons scattered by the pre-burst stellar wind.